Available online at www.sciencedirect.com
SCIENCE DIRECT®
Carbohydrate Research 340 (2005) 959–970
Carbohydrate RESEARCH

Hyaluronan chain conformation and dynamics

Sara Furlan,[a,†] Giovanni La Penna,[b,‡] Angelo Perico[b] and Attilio Cesàro[a,*]

[a]*Department of Biochemistry, Biophysics and Macromolecular Chemistry, UdR INSTM, University of Trieste, I-34127 Trieste, Italy*
[b]*Institute for Macromolecular Studies, Section of Genova, National Research Council, via De Marini 6, I-16149 Genova, Italy*

Received 13 October 2004; accepted 25 January 2005

Dedicated to Professor David A. Brant

Abstract—An overview of the present state of research in the field of hyaluronan chain conformational aspects is presented. The relationship between structure and dynamics are illustrated for a series of hyaluronan oligomers. Conformational characteristics of hyaluronan chains are discussed, together with the dynamic chain patterns, evaluated by using a theoretical approach to diffusive polymer dynamics. The dependence of correlation times and NMR relaxation parameters from the chain dimension are investigated. Topological features and dimensional properties are related to the structural determinants by using classical computational methods of molecular mechanics and Monte Carlo simulation.

Keywords: Hyaluronan; HA oligomers; Monte Carlo; Conformational energy; Local dynamics; Chain conformation

1. Introduction

In recent years, significant progress has been made in both the experimental and theoretical research tools needed to study the conformational complexity of carbohydrate polymers in solution,[1] using such methods as X-ray and neutron-scattering techniques (SAXS and SANS), atomic-force microscopy (AFM), high-resolution NMR spectroscopy and relaxation techniques, and computational methods. The prediction of conformational features has always been the main aim of molecular mechanics (MM) since the beginning.[2,3] Unrefined or semi-empirical force-fields have been used by several authors with the implicit assumption of possessing the most appropriate tool for this purpose. Leaving aside the ordered conformations of the secondary structures deduced by diffraction studies, several experimental (thermodynamic) averages have been, from time to time, proposed as suitable for comparison with models constructed by computational procedures. All experimental and computational methods unequivocally indicate the relevance of the monomer structure and linkage of environmental effects (such as, solvent composition, pH and salt conditions, and temperature) on the topological shape and properties of carbohydrate polymers.[4] The general problem of the solvent effect on conformational states, and preferential solvation of oligo- and poly-saccharides has been tackled mainly to validate detailed molecular models that were developed for relating the structural characteristics of these macromolecules to their chemical, physical, and biological properties in solution.[5] Even recently, however, semi-empirical methods have been shown very useful and are generally applicable to different chain linkages and monomer composition.[6,7]

In this paper we follow a protocol well established for the quantitative description of the size and shape of biopolymer chains (here, specifically hyaluronan, HA). This implies the construction of chain models by numerical

* Corresponding author. Fax: +39 040 558 3684; e-mail: cesaro@units.it
† On temporarily leave at Institute for Macromolecular Studies, Genova.
‡ Affiliated to the Magnetic Resonance Center, University of Firenze, Italy.

0008-6215/$ - see front matter © 2005 Elsevier Ltd. All rights reserved.
doi:10.1016/j.carres.2005.01.030

Monte Carlo simulation[8] on the basis of conformational statistical weights of representative dimeric units. However, for the first time (to the best of our knowledge) the force field used for the conformational energy landscape has been carefully calibrated and tested to fit the local dynamics of oligomeric chain segments.[9] In doing that, many approximations necessarily made within the dimer statistics are removed. To some extent, however, this approach is similar to other attempts that used different statistical equilibrium properties (like SAXS data in the case of pullulan[6,10]).

The paper is organized as follows. The next part provides a brief but essential summary of literature results on HA conformation, in order to establish the relevant background (more details are given in the review by Cowman in this issue[11]). The 'Computational Methods' section summarizes the methods to obtain the maps of glycosidic linkages, the statistical chains, and NMR relaxivities. A summary of the definitions of the parameters describing the conformations of HA oligomers and polymers is also included there. In the 'Results and Discussion' section, firstly the conformation of short UA oligomers is analyzed, then, the ^{13}C NMR relaxivities of $(UA)_n$ oligomers, with $n < 7$, are discussed in terms of conformational and frictional properties; and finally, the average chain parameters such as persistence length and radius of gyration are calculated and compared with literature data. In the 'Conclusions' section, implications and perspectives of this approach in the frame of the HA polymer are given.

2. A brief outlook on the conformational properties of hyaluronan

The relevance of hyaluronan (HA) in living organisms and in artificial biological systems has been emphasized and reported in many occasions.[12,13] This polysaccharide displays intriguing viscoelastic and conformational features, although it has a relatively simple regular structure, being an alternating copolymer with a disaccharide (U,A) repeat unit, {→4)-β-D-glucuronate-(1→3)-2-deoxy-2-acetamido-β-D-glucose-(1→}, as illustrated in Figure 1. There are several aspects of HA that make this molecule an interesting subject for investigation. The macromolecular properties of high molecular weight hyaluronan in dilute solution have been consistently interpreted[11] on the basis of a worm-like coil with moderate stiffness,[14] and more recently of a 'stiffish' coil[15] but an atomistic description of these properties has been elusive.

Although the present study does not deal with concentrated interacting chains, it is relevant to the discordant interpretation that has been given for the 'stickiness' of HA chains observed in solution (network-forming and laterally-aggregating behavior). Rheological properties[16,17] of hyaluronan solutions in several conditions of concentration, pH, ionic strength, and molecular weight, have been investigated in order to shed light onto the effects that might arise from conformational ordering. Several studies have suggested that the determining factors for conformation and packing in the solid state[18] also influence the hyaluronan chain in solution. In particular, the tendency to aggregation has been ascribed by some authors[19,20] to in-registry intermolecular and intramolecular interactions between the polysaccharide chains, but the formation of stable aggregates has been questioned.[21] In solution free of added electrolyte, HA forms polydisperse, entangled aggregates, which remain stable for weeks at a time, while in solutions of medium to high ionic strength, most of these aggregates disentangle within days.[22]

An extensive hydrogen-bonding network has been claimed by several authors for the secondary structure of hyaluronan in aqueous solution, which would give the polymer an overall expanded-coil structure. However, the actual effect of these interactions on the chain conformation has not been extended to more than short oligosaccharides, in a solid-like crystalline conformation. Another recent paper[17] suggested a detailed topological structure for the high molecular weight HA and unfractionated low molecular weight HA fragments in aqueous solution, on the basis of local structural information gained by ^{13}C NMR and X-ray fiber-

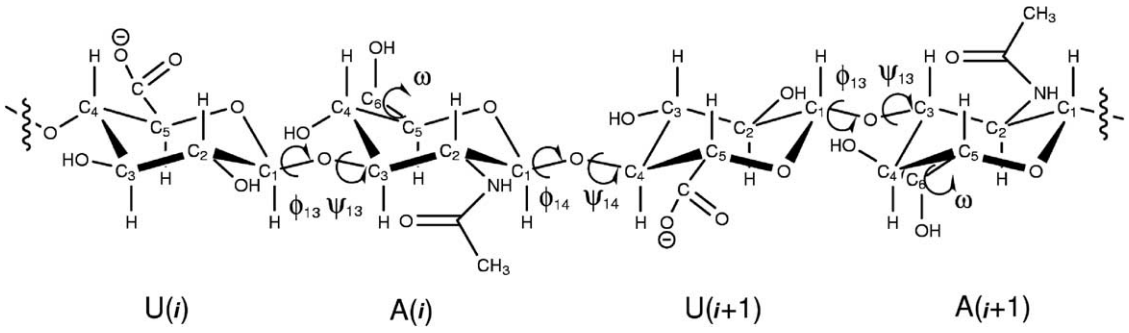

Figure 1. Schematic drawing of the tetrasaccharide (U(i)–A(i)–U(i + 1)–A(i + 1)) in HA chain. Main atomic position and torsion angles at the glycosidic linkages and C-6 atom are labeled.

diffraction data. This picture is in conflict with the old experimental data of scattering and intrinsic viscosity that suggest a moderate stiffness, namely, a persistence length L_p of about 5 nm.[14] Other authors[22] found that the total apparent persistence length varied from about 8.7 nm at the high ionic-strength limit to nearly 40 nm at 1 mM added NaCl, and this was considered to be consistent with the earlier knowledge of local stiffening. Almost similar conclusions were reached by recent investigations on fractionated samples of HA over a wide range of molecular weights (10^4–10^7), suggesting that the worm-like chain model with unmistakable semi-flexibility can be applied to this polymer. However, by using different theoretical models, slightly discordant values of L_p have been extracted, ranging from 4.2 to 10 nm.[11,23–28] Besides the lower values found by Hayashi et al.[23] and by Takahashi et al.[24] (4.2–4.5 nm, in 0.2 M NaCl) most of the other literature results show higher values. A persistence length of 8.5 nm was calculated by Fouissac et al.[25] in 0.3 M NaCl, while a value of 9–15 nm was reported in 0.15 M by Gamini et al.[26] More recently, Mendichi et al.[27] reported L_p = 9.5–9.8 nm for ultra-high molecular weight HA samples in 0.5 M NaCl and a smaller value (6.8–7.5 nm) for another set of samples with lower molecular weights (10^4–10^6). The dependence of L_p of worm-like polyelectrolytes on the salt concentration is well known, and may in part justify these differences. The most recent investigation[28] by static, dynamic, and small-angle neutron-scattering confirms the values for the intrinsic persistence length of the chain (i.e., $L_{po} \approx 9$ nm), and suggests that the total persistence length, $L_{pT} = L_{po} + L_{pe}$, is almost doubled in conditions of low ionic strength due to the electrostatic contribution to the L_{pe} term.

However, identification of the physical reasons for the conformational versatility of HA still elude a full molecular understanding. To this end both MD and NMR studies (or a combination of them) have recently been carried out.[29–40] Among experimental investigations, an NMR study[29] of the effects of various environmental conditions on the conformation of oligomeric and polymeric HA suggested that the conformational versatility of HA is related mainly to the averaging of conformational states at the glycosidic linkages. Other more recent MD and NMR studies have been mostly restricted to small oligomers, leaving out any flexibility and claiming a strict rigidity for both (1→3) and (1→4) linkages, 'due to direct and/or water mediated inter-residue hydrogen bonding'.[30] Whether this rigidity can be extended to the description of high molecular weight chains is undoubtedly questionable. Several other MD and NMR data suggest a dynamic stiffness modulated along the chain, because 'no one hydrogen bond exists for an extended period of time'.[31] Indeed, some other recent NMR investigations[32,33] addressed their attention specifically on dynamic parameters (relaxivities), providing a good comparison between experimental results and the simulations[34] discussed later.

As far as the computational studies are concerned, several MD simulation studies have been confined to very short oligomers (from disaccharides to tetrasaccharides).[30–32,34] The conformational freedom of hyaluronan di- and tetra-saccharides has been compared with available NMR data, stressing the importance of the hydrogen-bonding network, based both on direct intramolecular hydrogen-bonding and through water caging around the glycosidic linkage.[31] The combination of computer simulations with diffusion theory gives a microscopic description of the NMR relaxivities for biopolymers, without any approximations concerning the separation[35] or coupling between time scales.[36] Nevertheless, most of the MD applications to HA oligomers[30,32,37–40] did not involve a quantitative derivation of NMR parameters from MD trajectories, mainly because of the large errors in simulated time-correlation functions. Calculation of NMR relaxation parameters based on diffusion theory and mode-coupling approach (MCD theory, hereafter) were performed on HA oligomers.[34] The results showed that the method permits calculation, on a microscopic basis, of every 2nd-rank TCF in the molecule, once the configurational statistics have been modeled. Still more recently, the effects of hydrogen-bond networks, electrostatic interactions, and solvation effects combined with short-range torsional potential, have been taken into account by using numerical techniques to obtain the configurational statistics.[9,34] MD simulations provided both the dynamics of the variables and their statistical averages and distributions, by acquiring deterministic trajectories of every configurational variable in the canonical ensemble.

However, none of these MD simulations have been fully exploited to predict the conformational features of HA polymer. In other words, where quantitative data were available on a macromolecular scale no atomistic description was possible, and 'vice versa'. Most often, the bridging between results obtained either on small HA oligomers or on statistical (thermodynamic) averages has been ambiguously interpreted, as already mentioned, in terms of chain 'semi-flexibility', 'stiffness', 'rigidity', and 'stickiness'.

The foregoing summary was considered necessary in order to stress the importance of those studies that have provided the intrinsic key to reveal the molecular properties and the unique versatility of HA. This overview of the concepts on which present knowledge of the HA conformation is based leaves the impression that the gap between the local intra-residue conformational dynamics and the overall chain conformational shape has not yet been filled. Based on simplistic statistical considerations, the persistence of connecting inter-residue bridges

(as proposed on the basis of the recent studies) up to rather long oligomers does not appear to be straightforward, unless highly cooperative interactions are claimed. The main difficulty is the availability of both experimental dynamic data on suitable oligomers (longer than a tetrasaccharide) and dynamic simulation data on the whole series of homologues, from the short tetrasaccharide to the high molecular weight chains.

3. Computational methods

3.1. Nomenclature

Hyaluronan (HA) is made up of repeating disaccharide units each constituting β-D-glucuronic acid (GlcA) and 2-acetamido-2-deoxy-β-D-glucose (GlcNAc) linked (1→3) and (1→4), respectively (see Fig. 1). In this paper, these residues are labeled as U and A, respectively. Thus, the HA chains are indicated with $(UA)_n$ where n is the number of disaccharide units. In the calculation of dimensional properties (such as, the characteristic ratio $C_n = \langle r_0^2 \rangle / Nl^2$), however, the usual convention for copolymers has been used, with $N = 2n$ and the virtual bond l is given by the relation $l^2 = (l_U^2 + l_A^2)/2$.

The Φ and Ψ dihedral angles in the glycosidic linkages are defined as the dihedral angles between the bonds H-1(U)–C-1(U)–O-1(U)–C-3(A) and C-1(U)–O-1(U)–C-3(A)–H-3(A) for UA and H-1(A)–C-1(A)–O-1(A)–C-4(U) and C-1(A)–O-1(A)–C-4(U)–H-4(U) for AU, respectively, where the dihedral angle is 180° in the *trans* conformation.[2]

3.2. Choice of the force field

In our previous reports[9,34] the CHARMm force-field developed for saccharides was always used. In Ref. 9 the conformational maps of UA and AU dimers were reported, and from those maps statistical chains were generated, with average persistence length of about 20 nm (data not shown) using the same method described later. This value does not agree with the accepted experimentally estimated persistence length of about 9 nm. As observed in our previous paper, the high rigidity of this model for the HA chain is due to the inaccessibility of minima far from the absolute minimum in the conformational map. These energy minima are accessible at high temperature, and are expected to statistically increase the flexibility of the HA chain, inasmuch they provide more compact conformations. Therefore, the version of the CHARMm force-field used describes well the conformational wobbling around the conformations of larger stability (the global minimum), and is suitable for local dynamics and molecular-dynamics simulations. Nevertheless, a different force-field must be chosen when describing statistical properties that are sensitive to the presence of different minima in the conformational energy-map. A suitable test for the choice of such a force field is the construction of molecular chains according to the conformational maps of oligomers. Among the sets of parameters mentioned in the literature, and for the reasons outlined in the results, we have chosen to use the OPLS all-atom (OPLS-AA) force-field, whose parameters are available[41] and reported in published tables when used on carbohydrates.[42]

3.3. Generation of conformational maps

Energy maps of UA and AU dimers as functions of the Φ and Ψ dihedral angles of the glycosidic linkages were obtained through Monte Carlo (MC) simulated annealing (SA) trajectories of the all-atom OPLS models in vacuum of AUAU and UAUA tetrasaccharides, respectively. Description of simulations[9] and the program[43] used has already been reported.

Both UAUA and AUAU are composed of 95 atoms (all the atoms in the molecule). The dihedral angles in the pyranose rings were kept constant at their values initially set. For each set of Φ, Ψ dihedral angles in the glycosidic linkages, the other 24 dihedral angles were used as degrees of freedom. The carboxylate groups are all neutral in the adopted force field like in our previous papers.[9,34]

The electrostatic interactions were damped and shifted by using the charge neutralization approach,[44] so as to allow the use of a distance cut-off to speed-up simulations and to avoid the usual dependence of electrostatic potential-energy from the cut-off. Both Lennard–Jones and damped electrostatic interactions were smoothly switched off between 0.9 and 1.0 nm and the damping constant for electrostatic interactions was $2\ \mathrm{nm}^{-1}$.[9] A dielectric constant of 1 was used in the calculations.

The MC algorithm extracts the statistics from suggested configurational moves. These moves were obtained, as usual, in the torsional space by randomly modifying dihedral angles and keeping bond distances and angles constant, including the dihedral angles of pyranose rings. The bond distances and angles are kept fixed to equilibrium values, except for the glycosidic bending angle, which was fixed at 117°. The pyranose rings were always in the $^4C_1$ conformation.

One dihedral angle is randomly chosen within the set of variables and modified by applying a random displacement in the range $[0, \pm\pi]$. A MC sweep corresponds to the tentative modification of the entire set of variables. A Monte Carlo trajectory of 100,000 sweeps was performed for each pair of fixed Φ and Ψ glycosidic dihedral angles in the central linkage. The pair of dihedral angles was modified in steps of 10°. The temperature of the MC trajectory was exponentially

decreased according to rule $\beta = \beta_0(\beta_1/\beta_0)^{(i-1)/(N-1)}$ with $\beta = 1/k_BT$, i the current MC sweep, N the total number of MC sweeps, the initial temperature $T_0 = 1000$ K and the final temperature $T_1 = 100$ K. The potential-energy U corresponding to the minimum explored during the annealing was assigned to the corresponding point in the conformational map $U(\Phi, \Psi)$.

3.4. Generation of statistical chains

In order to evaluate the behavior and the dimensions of HA polymer chains in solution, in Θ conditions, samples of chains with n up to 500, that is, $(UA)_{500}$, were generated by using the Monte Carlo technique. In this calculation, the polymer chain is assembled residue by residue. The conformation of each glycosidic linkage along the chain is selected using the Metropolis algorithm from (Φ, Ψ, U) triads of UA and AU maps. This construction does not take into account interactions between atoms farther than four monosaccharides along the chain. Thus the excluded volume is not taken into account. Statistical Monte Carlo sampling of 20,000 chain conformation was performed at the temperature of 300 K by a program implemented in our laboratory. The topological properties, such as the unperturbed dimension and the stiffness of the oligomer and polymer chains, are described by quantities such as the mean end-to-end distance (h), the limiting value of the characteristic ratio (C_∞) and the persistence length (L_p):[3]

$$h(n) = (\langle |r(n)_0|^2 \rangle)^{1/2}, \tag{1}$$

where $r(n)$ is the distance in space between C-4(U) and C-1(A) atoms, n is the number of disaccharide residues, the angular brackets indicate an average ensemble over all the polymer chains, and the subscript '0' denotes the unperturbed conditions; the persistence length is defined as the projection of the end-to-end distance vector $\mathbf{r}(n)$ on the first residue UA, distance vector of the chain ($\mathbf{l}_1$):

$$L_p(n) = \langle (\mathbf{l}_1 \cdot \mathbf{r}(n)) \rangle / l_1; \tag{2}$$

finally,

$$C_n = h^2(n)/nl^2. \tag{3}$$

where l is the virtual bond length averaged over the residues U and A. L_p and C_∞ are the asymptotic values of $L_p(n)$ and $C(n)$, respectively, when n approaches infinity.

3.5. Calculation of NMR relaxivities

In this subsection we summarize the diffusion-approach theory[9,32,45] to be applied to the calculation of the NMR relaxivities.

Assuming that the ^{13}C nuclear spin relaxation is governed by the dipolar and chemical shift anisotropy mechanisms induced by the hydrogen atom bonded to ^{13}C, the relationships between the $R(C_z)$ relaxivities and spectral densities are:[46,47]

$$R(C_z) = dJ(\omega_H - \omega_C) + (3d + c)J(\omega_C) + 6dJ(\omega_H + \omega_C), \tag{4}$$

with

$$d = \frac{\gamma_C^2 \gamma_H^2 \hbar^2}{20}, \quad c = \frac{(\omega_C \delta)^2}{15} \tag{5}$$

γ_i is the gyromagnetic ratio of nucleus i, and δ is the (dimensionless) chemical shift anisotropy (CSA) of each C nucleus. In this work we have assumed that the CSA is -40 ppm for all the monitored C–H bonds.

The spectral densities J are the Fourier transform:

$$J(\omega) = 2\int_0^\infty \cos(\omega t)\mathrm{TCF}(t)\,\mathrm{d}t \tag{6}$$

of the time-correlation function (TCF) of 2nd-rank tensor components of the vector $\mathbf{r}$ joining the monitored ^{13}C nucleus with the bonded protons.

This TCF has the following form[47]

$$\mathrm{TCF}(t) = \left\langle \frac{1}{r^6} \right\rangle P_2(\cos[\theta(t)]), \tag{7}$$

with $\theta(t)$ is the angle spanned by the C–H vector in time t.

Integrating the orientational part of the TCF, the correlation time τ is obtained:

$$\tau = \int_0^\infty P_2(\cos\theta(t))\,\mathrm{d}t. \tag{8}$$

The mode-coupling diffusion (MCD) theory of the dynamics of a biological macromolecule in solution was adopted for the computation of the above TCF of Eq. 7. The approximations in the mode-coupling expansion solution of the Smoluchovski diffusion equation are the same as in the previous application to HA oligomers in Refs. 9 and 34.

For time-correlation functions of 2nd-rank tensor components, such as those necessary to calculate NMR relaxation (see Eq. 4) the reduced 2nd-order basis set RM2-II[48] is generated coupling the 1st-order/1st-rank modes in the proper irreducible tensorial form up to the fourth power. Let e be the number of the lowest-rate 1st-order/1st-rank modes that we choose. The RM2-II basis set contains $e(e+1)/2$ second powers and $[e(e+1)/2]^2$ fourth powers of these e 1st-rank/1st-order modes. Once the 2nd-rank TCFs have been generated, they can be Fourier transformed to obtain the spectral densities, which turn out to be sums of Lorentzian functions.

The diffusion theory treats the solvent hydrodynamically and uses a detailed molecular model for the polymer in terms of beads (atoms or groups of atoms) connected by real or effective bonds diffusing in an atomistic potential (the same potential used in the

simulation). The beads are represented as points of coordinates $\mathbf{r}_i$ with friction coefficients $\zeta_i = 6\pi\eta a_i$, where η is the solvent viscosity. In this work, the choice of hydrodynamic parameters (Stokes radii, friction location, and hydrodynamic screening constant α) are identical to the previous application of MCD theory to the $(UA)_4$ HA oligomer.[9,34] Summarizing, the friction points are located on most of the heavy atoms in each monomer for a total amount of 22 friction points for each UA dimer. Each bead represents isotropically the friction of the heavy atom together with the bonded hydrogen atoms. The Stokes radii of the beads are derived by the zero-probe accessible surface area (ASA) of the group of atoms centered on each bead. The radii are within 0.073 nm (the single O-1 atom) and 0.185 nm (the methyl group of residue A). The screening constant α in Eq. A7 in Ref. 9 is 0.25.

In the RM2-II basis-set, values up to $e = 10$ were used, in order to test the convergence of dynamical quantities. The values of $e = 5$, 7, 9, 10 were used for $(UA)_2$, $(UA)_3$, $(UA)_4$, $(UA)_7$, respectively.

4. Results and discussion

4.1. Conformational maps and residue conformations

The first step in the computational work is the evaluation of the conformational energy maps for the rotations Φ and Ψ for the two glycosidic linkages UA and AU. This goal has been done by using the two tetrasaccharides (i.e., AUAU and UAUA segments, respectively). Such a choice was indicated by the observation that the addition of next neighbors to the disaccharides involved in the glycosidic linkage leads to a significant effect of long-range interactions.[49] Based on our previous work on the octasaccharide $(UA)_4$,[9] the configurational statistics and the dynamical relaxivities of this short oligomer were nicely matched both by MD simulation and by the 'refined' force field used here. This force field compensates medium-range and solvent interactions, providing a good approximation to experimental dynamical results. Moreover, the net charge of carboxylate groups has been assumed to be zero. Under such circumstances, the resulting chain model is in the unperturbed conditions (Θ-solvent), inasmuch as only short-range interactions are included, without any account for excluded volume effect.

In Figure 2, the potential-energy surfaces obtained by the MC simulated annealing are displayed as contour plots for the UA and AU linkages (panels a and b, respectively). The overall shape of both maps in the region close to coordinates 0,0 (region A in the figures) is similar to previous results obtained on HA oligomers based on the CHARMm force-field.[9,32,35] The UA linkage displays a single minimum in region A (Fig. 2 panel a), while the AU linkage displays two close and broad minima in region A and another sharp minimum in region B. Other slightly significant regions are marked on the maps, that may occasionally contribute on a large scale statistics. As already discussed,[35] the difference of the two maps is consistent with a wider wobbling of AU glycosidic dihedral angles compared to that of UA. Furthermore, in the case of the AU linkage the two minima in this region correspond to the inter-residue hydrogen bonds O-5(A)–HO-3(U) formation that enhances the stability of the conformation at about $(30, -10)$. In general, all the findings here reported agree

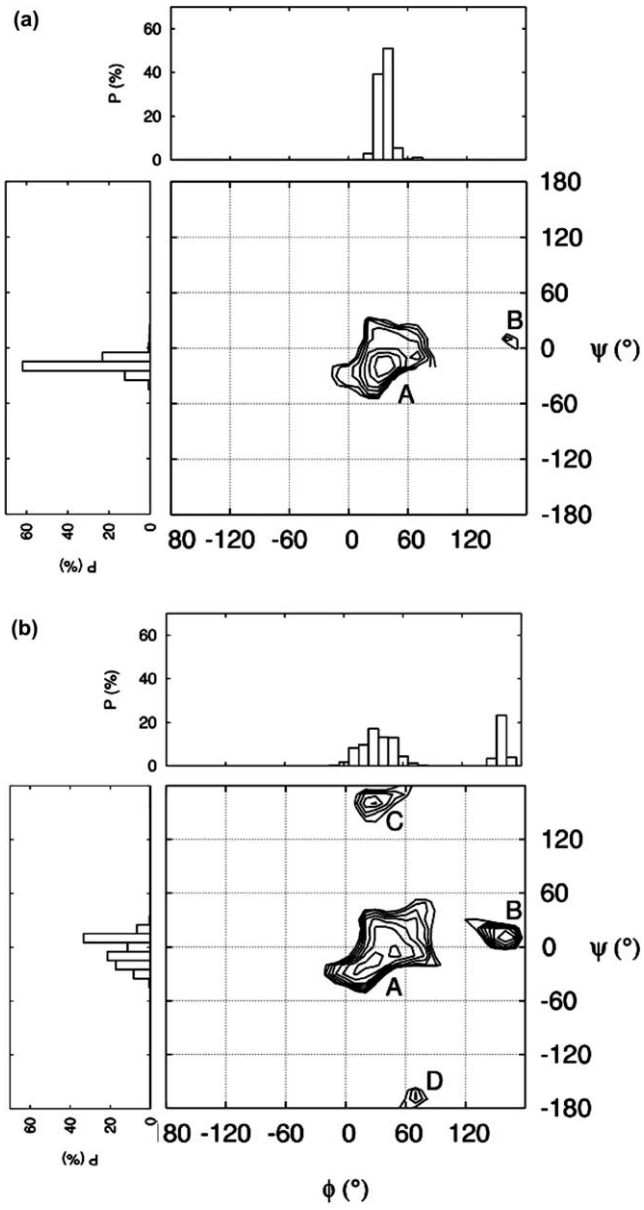

Figure 2. Conformational maps of **AUAU** (a) and **UAUA** (b) tetramers with fixed and dihedral angles in the central glycosydic linkages. Contour levels are at 1.0, 2.0, 3.0, 4.0, 5.0, 6.0, 7.0 kcal/mol with respect to the absolute minimum calculated for each map. Population densities at 300 K are projected of left and top axes.

fairly well with the computational results of recent literature.

In order to provide a quantitative estimation of the inherent flexibility of glycosidic linkages, the angular distribution of population (at 300 K) for each glycosidic angle is projected on top and left axes (Fig. 2). Comparison of the angular distribution provides a further (if necessary) indication of the difference above discussed and of its effect on the dynamical wobbling properties (see later). The most striking difference in conformational maps, that is observed by using the OPLS-AA force-field compared to the previous results, is the presence, in the AU linkage, of several low-energy minima that contribute to more compact oligomer structures.[9] The potential-energy minima are identified and labeled in Tables 1 and 2. The global (although less populated) minimum of the AU conformational map is now displaced in a region with Φ close to 180° and a further minimum with energy of about 3 kcal/mol higher than the global minimum is also present. Minima were found in these regions for the AU linkage also by using the CHARMm force-field, but in this latter case the energy differences between these minima and the global one were of the order of 9 kcal/mol. Therefore, compact structures were accessible only at very high temperature (1000 K).

Figure 3 shows some snapshots of segments AUAU and UAUA taken as representatives of the conformations of the central linkages (UA and AU, respectively) populating the most relevant minima (see Fig. 2 and Tables 1 and 2). In general, as it has been already found in the detailed modeling of the conformational wobbling in the regions A of both type of linkages, the energy landscape is strongly influenced by hydrogen bonds, and these hydrogen bonds play a major role in the topological definition of AU and UA linkages. Focusing on the central linkage in the two tetrasaccharides, the first panel (Fig. 3a) shows the molecular topology of the tetrasaccharide AUAU, putting in evidence the inter-residue hydrogen bond between atoms O-5(U) and HO-4(A). This interaction is likely to occur for most of conformational states of region A, as it can be observed also in the other snapshots (Fig. 3b, c, and d) where the linkage UA is at both ends of the tetrasaccharide UAUA.

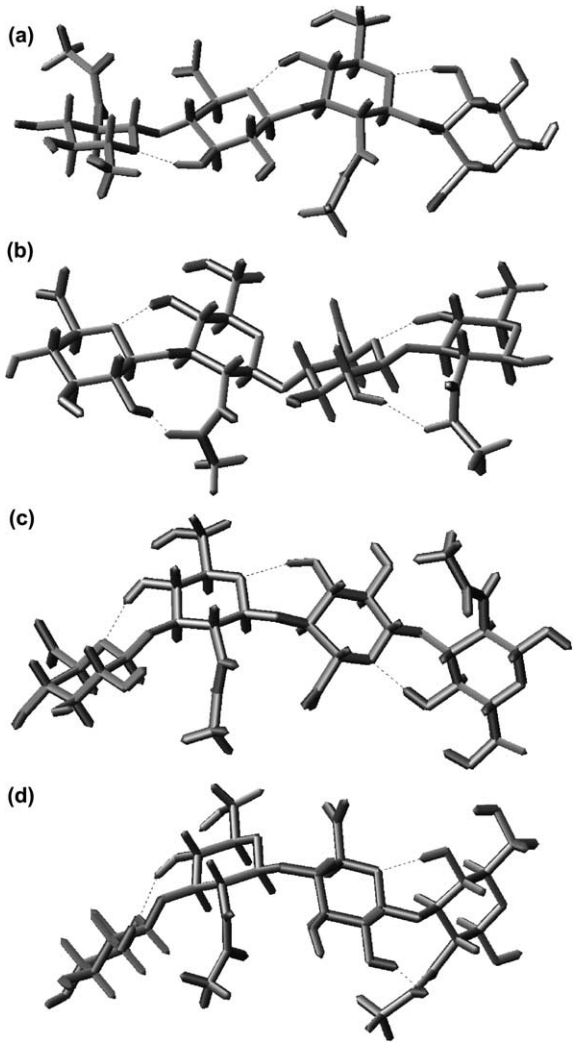

Figure 3. Representative snapshot of tetramer conformational features in the minima defined in Figure 2; (a) conformation of tetramer AUAU in the minimum A; (b), (c), and (d) conformations of tetramer UAUA in the minima A, B, and C, respectively. The snapshots have been printed with the program MOLMOL.[50]

Table 1. Minima of the potential-energy surface of the linkage **UA** in the tetrasaccharide A**UA**U

	A	B
ϕ (deg)	40	160
ψ (deg)	−20	10
(kcal/mol)	0.00	5.19
Population of region (%)	99.99	0.01

Table 2. Minima of the potential-energy surface of the linkage **AU** in the tetrasaccharide U**AU**A

	A	B	C	D
ϕ (deg)	30	160	30	70
ψ (deg)	−10	10	160	−170
(kcal/mol)	0.00	−0.60	2.25	4.26
Population of region (%)	69.05	30.63	0.31	0.01

The situation is rather more flexible for the linkage AU. The three snapshots (Fig. 3b, c, and d) have been taken with the local conformation of the central residue AU exploring the three minima identified in Figure 2b as A, B, and C, respectively (minimum D has not been given any significance in this context). Only for the AU linkage populating minimum A, a hydrogen bond between atoms O-5(A) and HO-3(U) is formed, thus stabilizing this conformation. The secondary region B is also highly populated, despite the absence of hydrogen bonds and a linkage conformation, that is, generally considered less favorable. The occasional formation of a hydrogen bond involving HO-2(U) and the carbonyl

oxygen in the amide group of the residue A surely provides an additional stability to the conformations depicted in Figure 3c and d. This hydrogen bond, that was already reported in all-atom MD simulations,[37] is forbidden in the A region because the methyl group in the A side chain clashes with the U residue.

Whether the stability of conformational region B in the tetrasaccharide arises from the contribution of more favorable interactions of the nearest residues alone, or by other less clear topological effects, is matter for further investigation. In any case, however, this has been the main reason for using the tetrasaccharide segments to model HA chains.

4.2. NMR relaxation

The configuration statistics allows computation of the statistical averages in the MCD theory and, therefore, the numerical computation of the NMR parameters. Therefore, the combination of conformational maps and diffusion theory offers a very valuable tool to compare the essential features of the force field with experimental data routinely measured by NMR for carbohydrate oligomers and polymers. At variance with the previous applications of the diffusion theory, we have computed here the $R(C_z)$ relaxivities on the basis of the statistics derived by the $(UA)_{500}$ chains, generated by MC according to the conformational maps. Therefore, within the assumptions of these statistics, it is possible to monitor NMR relaxivities as functions of the position of C nuclei in the chain as well as of the number of disaccharide units n in the chain.

In Figure 4 NMR relaxivities are displayed together with the correlation times τ that summarize the mobility of C–H bonds (right y axis). Both relaxivities and correlation times are averaged within the ring carbon atoms belonging to each residue U (left panels) or A (right panels), respectively. The residues U and A at the nonreducing end (top panels, a and b) and at reducing end (bottom panels, e and f), respectively, have been separated from the internal residues of the chains (mid panels, c and d). This classification has been adopted in order to simplify the comparison with NMR data that are reported in a similar scheme.[33] The relaxivities computed with this HA model are within 25% of the experimental data, and in all cases they are larger than in the experiments. Although the many approximations involved in the model (namely, neglecting the solvent and excluded volume effects, and neglecting statistical correlation between linkages farther than four saccharides), the calculations may be considered to offer fair agreement with experiments. As a matter of fact, a slight increase of the hydrodynamic interaction strength could compensate almost completely for these differences. A value of α less than 1 is related to the hydrodynamic approximations in the model, that is, it is related to the water solvation of sugars, and it is best determined by comparison of MCD calculations with experimental data for different oligomers: the value $\alpha = 0.25$ was fixed in previous work on the data of only two oligosaccharides.

The number ($n = 2$, 3, 4, and 7) of data is still limited for a detailed description of the different behaviors of internal and terminal relaxivities with the number of residues. In particular the important case $n = 7$ is probably underestimated because the mode-coupling expansion did not reach convergence at $e = 10$, due to the length of calculations. Nevertheless it can be appreciated as a fairly qualitative agreement in all cases with experiments.

The most important issue emerging from the NMR measurements of $R(C_z)$ is the number of disaccharide units in the oligomer for which the relaxivity is the same as in the polymer.[33] This parameter, also called 'critical length', depends on the NMR spectrometer frequency and on the molecular structure. The experiments on HA oligomers, as reported in the literature, show that HA has a critical length of three disaccharide units at 75 MHz, that is, similar to that of such rigid oligomers as cellulose triacetate (3.5 disaccharide units). Our calculations show a similar trend, namely, a critical length of about 3–4 units (see Fig. 4, panels c and d), as the relaxivity of central residues starts to decrease (as in the experiments) beyond 4 units. Nevertheless, larger oligomers must be included in the calculations in order to better extrapolate this discriminant quantity related to the polymer stiffness.

The interpretation of this critical length in terms of mobility is not straightforward. It may be noted that the correlation time for internal residues increases linearly as a function of n. Thus, the mobility depends roughly on n, while the relaxivity is almost constant or even decreases. On the other hand, the correlation time of terminal residues becomes constant beyond 4 disaccharide units, as expected for bonds less correlated with the main chain. The behavior of relaxivities at a given NMR frequency comes from an interplay between relaxation rates and amplitudes (order parameters). This effect does not permit extraction of direct information on mobility from single NMR experiments, but great help would come from relaxation measurements at different magnetic fields. In this latter case, the dependence of the critical length for internal residues from the magnetic field would give a strict constraint to the molecular structure and thus to the force field.

4.3. Chain statistics

Following the MC method described in Section 3.4, the statistical chain parameters have been calculated as a function of chain length n. The statistical sampling over 2×10^4 chain conformations has been considered sufficient for numerical evaluation of the averages of the

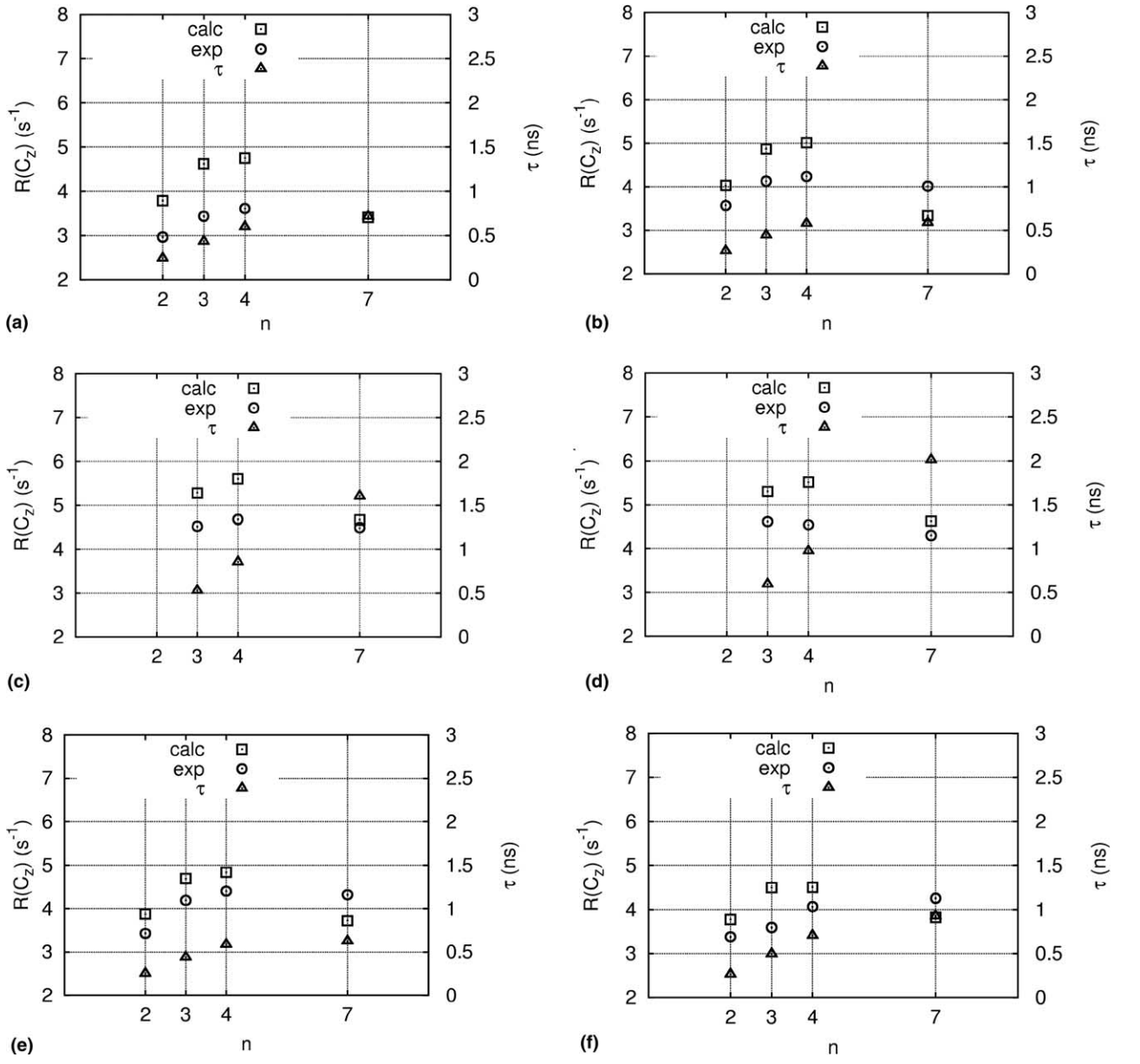

Figure 4. NMR $R(C_z)$ relaxivities at $\nu(^{13}C) = 75$ MHz, calculated (calc) and experimental (exp), and correlation times τ (right y-axis) as a function of n, number of disaccharide units. Both relaxivities and correlation times are averaged within the ring carbon atoms of each residue U and A. Panels show values for residue U and A, respectively: (a) and (b) nonreducing end, (c) and (d) internal residues, and (e) and (f) reducing end.

end-to-end distance h, radius of gyration R_g, persistence length L_p, and of chain characteristic ratio C_n.

These quantities are plotted in Figure 5a and b; the typical asymptotic behavior is observed for both trends of C_n and L_p. Above the value of chain length $n > 200$, the statistical gaussian regime is reached. At lower chain lengths, the departure from gaussian behavior is better appreciated from the plots reported in Figure 6a, where the ratio of the square end-to-end distance to the square of radius of gyration ($\langle r^2\rangle/R_g^2$) departs from the theoretical value of 6 at low n. The slow decrease of this ratio as a function of n, associated with a slightly bimodal trend in the variation of C_n and L_p with n, supports the concept of an 'intrinsic stiffness at nano-scale length' in the polymeric HA chain. As opposite to a continuous worm-like model this behavior arises from a random occupancy of secondary minimum B of the residues AU.

For a typical HA polymer with molecular weight of about 1.6 times 10^5 ($n = 400$), although ($\langle r^2\rangle/R_g^2$) ≈ 6.2, the chain can be thought to assume the statistical random-coil behavior. Such a chain exhibits a value of the characteristic ratio $C_n = 25.5$, with $R_g = 30.3$ nm and $L_p = 8.2$ nm (Fig. 5). Although several values are reported in the literature for the persistence length of hyaluronan, the discrepancy seems to arise from the difference in the ionic strength and in the corrections

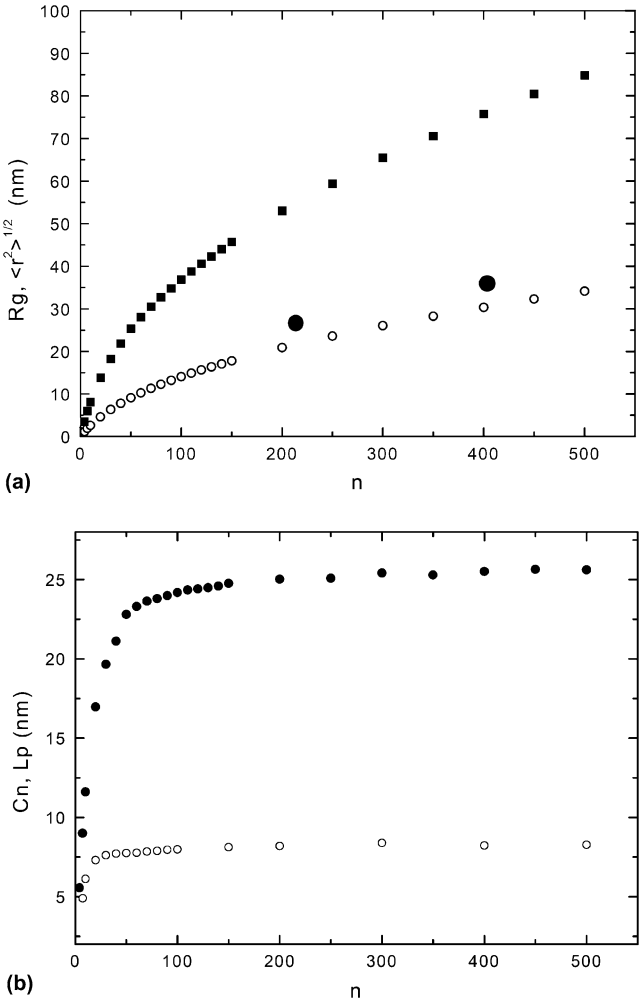

Figure 5. Chain dimension parameters as function of n, number of disaccharide units. Panel (a) averages of the end-to-end distance h (■), radius of gyration R_g (○), exp. values from Ref 28. Panel (b) chain characteristic ratio C_n (●) and persistence length L_p (○).

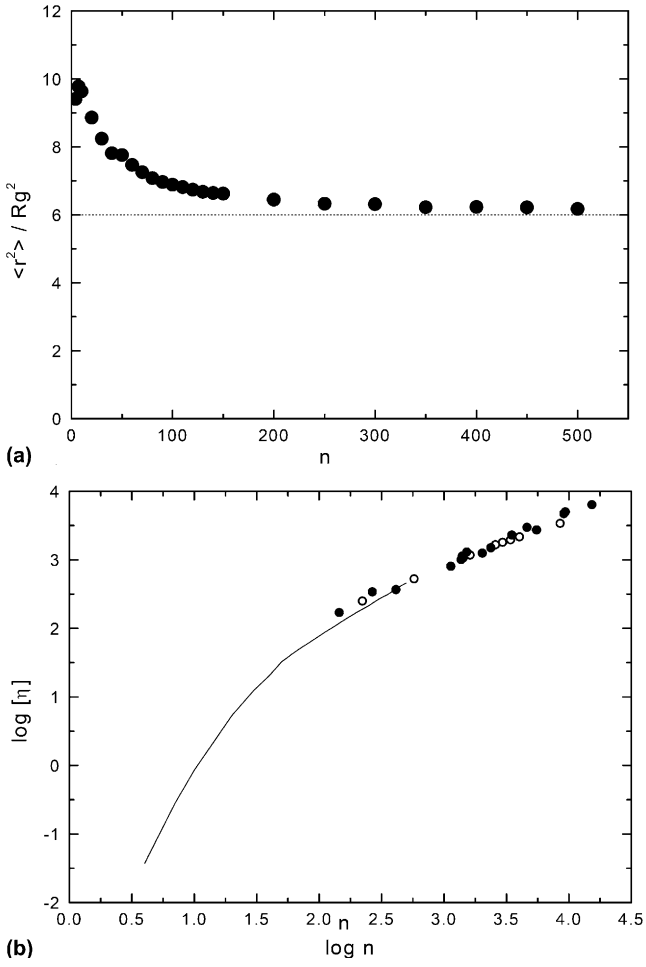

Figure 6. (a) Ratio of the square end-to-end distance to the square of radius of gyration ($\langle r^2\rangle/R_g^2$) as a function of n: departure from the theoretical value of 6 at low n shows the nongaussian behavior. (b) Double logarithmic plot of intrinsic viscosity as a function of n: the line is calculated from C_n–n dependence and data point are taken from literature.[27,28]

for polydispersity and for the excluded volume effect.[11] Thus, the value of the persistence length is in good agreement with the experimental values, which are in the range within 7 and 9 nm.[26–29] In particular, the calculated values of R_g and L_p for $n = 400$ differ slightly from the experimental findings of Buhler and Boué[28] (R_g = 35 nm (±4) and L_{po} = 9 nm), for HA polymer with same molecular weight (1.6×10^5) in 0.1 M NaCl. Taking for granted that the computation refers to Θ solvent and that all other conditions match the assumptions implicit in the comparison of these data, then an expansion coefficient $\alpha^2 = 1.3$ could be calculated. This comparison, however, is not made to provide the expansion coefficient itself, but rather to underline that, under these circumstances, the HA chain parameters have close similarity with those obtained in aqueous solution with a good screening of fixed charges. Additional relevant data for the polymer chains are the limiting values of L_p and C_n for $n \to \infty$, 8.25 nm and 25.6, respectively, that differ almost insignificantly from the data just reported for n = 400. Therefore, the present computational study assigns the HA polymer realistic conformational parameters, putting this polysaccharide stiffness on atomistic and more quantitative grounds.

Still more interesting is the prediction that the chain assumes different statistical behavior going from low to high molecular weight, according to the coefficient that scales the size with molecular weight of the polymer. A double logarithmic plot (Fig. 6b) has been constructed with the viscosity number of HA model chains calculated by using the Flory–Fox relation[51] that relates hydrodynamic and structural parameters of the chain. The numerical values of C_n calculated here and of $M = n \times 410$ have been used. The exponent of the power law (here the slope) changes from 0.55 at high molecular weight to the limiting value of about 1.8 for short oligomers ($n < 7$). Experimental data from literature[27,28] have been added in the same plot, in order to

scale the two trends and give significance to the calculated data.

Inspection of chain conformations randomly selected within the statistics of $(UA)_{n=500}$ is highly informative, as snapshots of these long chains can be visually compared with AFM HA images in a liquid aqueous layer, such as those obtained by Cowman and co-workers.[52] Four snapshots are provided in Figure 7, for visualization and comparison purposes (note that the 3D images are projected into the 2D plane of the figure, giving apparent chain overlapping). These chains display short elongated regions connected by sections with either worm-like character or with a higher degree of folding. Statistical conformational disorder, mainly due to the population of region B in the AU linkage, brings the elongated chain to an overall moderate folding. This type of folding should be rather sensitive to the environmental conditions, as conformational shift and new hydrogen bonds can occur with the result of a severe chain stiffening. It should be also noticed that a larger persistence length of about 20 nm is obtained by using within the same approach the CHARMm force-field (data not shown). This significant effect is mainly due to the very low population of energy minima corresponding to more compact conformations of the glycosidic linkages (i.e., conformations far from region A). There is not a single parameter in the force-field that can be addressed in producing this larger stiffness for the oligomers and, for the polymer therefore, in Θ conditions. Nevertheless, on average the CHARMm force-field contains larger van der Waals radii for several atoms, thus suggesting that a slight reduction of steric repulsions may give access to energy minima associated to hydrogen-bond networks otherwise forbidden at room temperature.

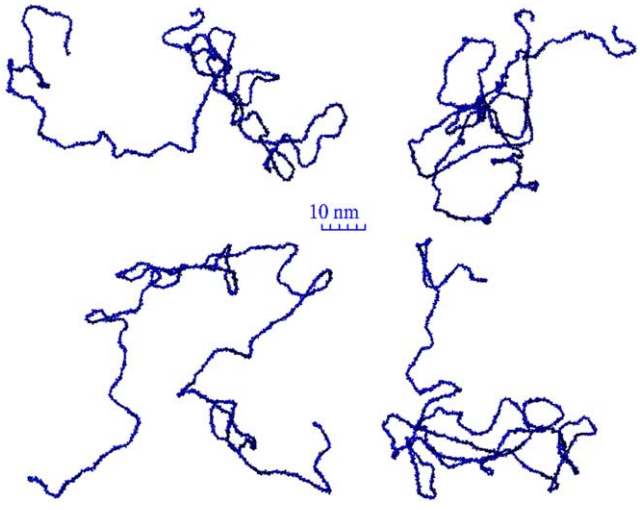

Figure 7. Four representative examples of the $(UA)_{500}$ chain conformation. The snapshots were printed with the program MOLMOL.[50]

5. Conclusions

The following conclusions and comments can be made:

- The computational procedure of the HA chain parameters was accomplished by using conformational energy maps that have been tested to reproduce satisfactorily both the dynamic properties of short HA oligomers and average chain-conformational properties up to 1000 saccharidic units. In this way, after scrutiny of several available force-fields, results that substantially agree with the most recent experimental observations on HA oligomers and polymer have been obtained.
- The peculiar short-range stiffness of the chain has been characterized by identifying the value of persistence length L_p and the variation of the dimensional and conformational properties with the chain length (namely, molecular weight). Pictorial snapshots of HA oligomers and polymers have also been generated. The contribution of several hydrogen bonds to the chain stiffness has been quantified.
- As far as the possibility of generalization of the procedure used here, a further comment seems necessary. The method relies on the diffusion theory that treats the solvent hydrodynamically and uses a detailed molecular model for the polymer in terms of beads connected by real or effective bonds diffusing in an atomistic potential. The fair success of describing dynamic and conformational properties of a moderately stiff chain, such as that of HA, is counterbalanced by limitations in the necessary MCD basis set for adopting the same strategy to much more flexible polysaccharides, such as pullulan (unpublished results).

References

1. Brant, D. A. *Curr. Opin. Struct. Biol.* **1999**, *9*, 556–562.
2. Brant, D. A.; Goebel, K. D. *Macromolecules* **1975**, *8*, 522–530; Brant, D. A. *Quart. Rev. Biophys.* **1976**, *9*, 527–596.
3. Mattice, W. L.; Suter, U. W. *Conformational Theory of Large Molecules*; Wiley: New York, USA, 1998.
4. Rees, D. *Polysaccharides Shapes*; Chapman & Hall: London, UK, 1977.
5. Dwek, R. A. *Chem. Rev.* **1996**, *96*, 683–720.
6. Liu, J. H.-Y.; Brameld, K. A.; Brant, D. A.; Goddard, W. A., III. *Polymer* **2002**, *43*, 509–516.
7. Ueda, K.; Ueda, T.; Sato, T.; Nakayama, H.; Brady, J. W. *Carbohydr. Res.* **2004**, *339*, 1953–1960.
8. Jordan, R. C.; Brant, D. A.; Cesàro, A. *Biopolymers* **1978**, *17*, 2617–2632.
9. Furlan, S.; La Penna, G.; Perico, A.; Cesàro, A. *Macromolecules* **2004**, *37*, 6197–6209.
10. Jaud, S.; Tobias, D. J.; Brant, D. A., personal communication (paper submitted).
11. Cowman, M. K.; Matsuoka, S. *Carbohydr. Res.* **2005**, *340*, doi:10.1016/j.carres.2005.01.022.

12. Lapacik, L. J.; Lapacik, L.; Smedt, S. D.; Demeester, J. *Chem. Rev.* **1998**, *98*, 2663–2684.
13. Hyaluronan 2003 Conference, (Cleveland, OH), Proceedings available at http://matrixbiologyinstitute.org/ha03/toc.htm.
14. Cleland, R. L. *Biopolymers* **1984**, *23*, 647–666, and references cited therein.
15. Hokputsa, S.; Jumel, K.; Alexander, C.; Harding, S. E. *Carbohydr. Polym.* **2003**, *52*, 111–117.
16. Morris, E. R.; Rees, D. A.; Welsh, E. J. *J. Mol. Biol.* **1980**, *138*, 383–400.
17. Scott, J. E.; Heatley, F. *Proc. Natl. Acad. Sci. U.S.A.* **1999**, *96*, 4850–4855.
18. Rao, V. S. R.; Qasba, P. K.; Balaji, P. V.; Chandrasekaran, R. *Conformation of Carbohydrates*; Harwood Academic: Amsterdam, The Netherlands, 1998.
19. Scott, J. E. *The Biology of Hyaluronan; Ciba Foundation Symposium 143*; Wiley: Chichester, UK, 1998.
20. Turner, L. R.; Lin, P.; Cowman, M. K. *Arch. Biochem. Biophys.* **1988**, *265*, 484–495.
21. Gribbon, P.; Heng, B. C.; Hardingham, T. E. *Biochem. J.* **2000**, *350*, 329–335.
22. Reed, C. E.; Li, X.; Reed, W. F. *Biopolymers* **1989**, *28*, 1981–2000; Ghosh, S.; Li, X.; Reed, C. E.; Reed, W. F. *Biopolymers* **1990**, *30*, 1101–1112.
23. Hayashi, K.; Tsutsumi, K.; Nakajima, F.; Norisuye, T.; Teramoto, A. *Macromolecules* **1995**, *28*, 3824–3830.
24. Takahashi, R.; Kubota, K.; Kawada, M.; Okamoto, A. *Biopolymers* **1999**, *50*, 87–98.
25. Fouissac, E.; Milas, M.; Rinaudo, M.; Borsali, R. *Macromolecules* **1992**, *25*, 5613–5617.
26. Gamini, A.; Paoletti, S.; Zanetti, F. In *Laser Light Scattering in Biochemistry*; Harding, S. E., Sattelle, D. B., Bloomfield, V. A., Eds.; The Royal Society of Chemistry: Cambridge, 1992; pp 294–311.
27. Mendichi, R.; Schieroni, A. G.; Grassi, C.; Re, A. *Polymer* **1998**, *39*, 6611–6620; Mendichi, R.; Soltes, L.; Schieroni, A. G. *Biomacromolecules* **2003**, *4*, 1805–1810.
28. Buhler, E.; Boué, F. *Eur. Phys. J. E* **2003**, *10*, 89–92; Buhler, E.; Boué, F. *Macromolecules* **2004**, *37*, 1600–1610.
29. Cowman, M. K.; Hittner, D. M.; Feder-Davis, J. *Macromolecules* **1996**, *29*, 2894–2902.
30. Donati, A.; Magnani, A.; Bonechi, C.; Barbucci, R.; Rossi, C. *Biopolymers* **2001**, *59*, 434–445.
31. Almond, A.; Brass, A.; Sheehan, J. K. *Glycobiology* **1998**, *8*, 973–980; Almond, A.; Brass, A.; Sheehan, J. K. *J. Mol. Biol.* **1998**, *284*, 1425–1437; Almond, A.; Sheehan, J. K. *Glycobiology* **2003**, *13*, 255–264.
32. Cavalieri, F.; Chiessi, E.; Paci, M.; Paradossi, G.; Flaibani, A.; Cesàro, A. *Macromolecules* **2001**, *34*, 99–109.
33. Cowman, M. K.; Feder-Davis, J.; Hittner, D. M. *Macromolecules* **2001**, *34*, 110–115.
34. Letardi, S.; La Penna, G.; Chiessi, E.; Perico, A.; Cesàro, A. *Macromolecules* **2002**, *35*, 286–300.
35. Holmbeck, S. M. A.; Petillo, P. A.; Lerner, L. E. *Biochemistry* **1994**, *33*(3), 14246–14255.
36. Kaufmann, J.; Möhle, K.; Hofmann, H.-J.; Arnlod, K. *J. Mol. Struct.* **1998**, *422*, 109–121.
37. Almond, A.; Brass, A.; Sheehan, J. K. *J. Phys. Chem. B* **2000**, *104*, 5634–5640.
38. Tafi, A.; Manetti, F.; Corelli, F.; Alcaro, S.; Botta, M. *Pure Appl. Chem.* **2003**, *75*, 359–366.
39. Prompers, J. J.; Scheurer, C.; Brüschweiler, R. *J. Mol. Biol.* **2001**, *305*, 1085–1097.
40. Tugarinov, V.; Liang, Z.; Shapiro, Y. E.; Freed, J. H.; Meirovitch, E. *J. Am. Chem. Soc.* **2001**, *123*, 3055–3063.
41. The OPLS parameters are available on request from Prof. W. L. Jorgensen at bill@adrik.chem.yale.edu.
42. Damm, W.; Frontera, A.; Tirado-Rives, J.; Jorgensen, W. L. *J. Comput. Chem.* **1997**, *18*, 1955–1970.
43. La Penna, G. *J. Chem. Phys.* **2003**, *119*, 8162–8174.
44. Wolf, D.; Keblinski, P.; Phillpot, S. R.; Eggebrecht, J. *J. Chem. Phys.* **1999**, *110*, 8254–8282.
45. La Penna, G.; Genest, D.; Perico, A. *Biopolymers* **2003**, *69*, 1–14.
46. Peng, J.; Wagner, G. *J. Magn. Res.* **1992**, *98*, 308–332.
47. Cavanagh, J.; Fairbrother, W. J.; Palmer, A. G., III; Skelton, N. J. *Protein NMR Spectroscopy*; Academic: San Diego, USA, 1996.
48. La Penna, G.; Pratolongo, R.; Perico, A. *Macromolecules* **1999**, *32*, 506–513.
49. Haxaire, K.; Braccini, I.; Milas, M.; Rinaudo, M.; Perez, S. *Glycobiology* **2000**, *10*, 587–594.
50. Koradi, R.; Billeter, M.; Wüthrich, K. *J. Mol. Graph.* **1996**, *14*, 51–55, http://www.mol.biol.ethz.ch/wuthrich/software/molmol.
51. Flory, P. J.; Fox, T. G. *J. Am. Chem. Soc.* **1951**, *73*, 1904.
52. Cowman, M. K.; Li, M.; Balazs, E. A. *Biophys. J.* **1998**, *75*, 2030–2037; Cowman, M. K.; Li, M.; Dyal, A.; Balazs, E. A. *Carbohydr. Polym.* **2000**, *41*, 229–235.